PHYSICS AND CHEMISTRY OF SOLID STATE
V. 25, No. 4 (2024) pp. 801-810
Section: Physics

DOI: 10.15330/pcss.25.4.801-810

Vasyl Stefanyk Precarpathian National University

ФІЗИКА І ХІМІЯ ТВЕРДОГО ТІЛА
Т. 25, № 4 (2024) С. 801-810
Фізико-математичні науки

PACS: 81.07.Wx; 81.20.Fw

ISSN 1729-4428 (Print)
ISSN 2309-8589 (Online)

Areej Adnan Hateef[1], Essebti Dhahri[2], Mohammed Rasheed[3], Habiba Kadhim[1], Zahraa Abbas[1], Noor Hassan[4]

Study of the influence concentration difference of copper in properties of cerium nanopowder

[1]*Authority of Scientific Research, Ministry of Higher Education and Scientific Research, Baghdad, Iraq,* tona96943@gmail.com
[2]*Laboratory de Physics Application, collage of Sciences, University Sfax, Tunis*
[3]*Applied Sciences Department, University of Technology, Baghdad, Iraq*
[4]*Dental Department, University of Kufa , Iraq*

Nano-pure cerium oxide CeO_2 nanopowder was prepared using the sol-gel method. The purity of the resulting powder was examined, and then copper impurities were added at concentrations of 3%, 6%, and 9% to the nano cerium oxide to enhance its structural and optical properties in order to achieve the best physical characteristics. Finally, the prepared pure and doped samples were tested as antibacterial agents against multiple strains of both Gram-positive and Gram-negative bacteria. The results of this work indicate that the CeO_2:Cu nan powders possess significant antibacterial properties, as they demonstrated the highest level of suppression against various pathogenic bacteria, suggesting future applications of CeO_2:Cu in nanobiotechnology as a biomaterial.

Keywords: Cerium oxide, sol-gel, nanopowder, Energy gap, antibacterial growth.

Received 28 July 2024; Accepted 18 November 2024.

Introduction

Cerium oxide (CeO_2) is a stable, rare, and active oxide [1] that is low cost and environmentally benign [2]. Oxidation states of cerium are tetravalent (Ce^{4+}) and trivalent (Ce^{3+}), in two oxide forms are CeO_2 and Ce_2O_3, respectively [3]. CeO_2 has huge applications such as; biosensing [4], antibacterial [5], solar cells [6], corrosion inhibition [7], gas sensing [8], photoactivity [9], supercapacitor [10]. Cerium dioxide has attracted significant attention due to its excellent photochemical stability [11], non-toxicity, low cost [12], and excellent biocompatibility [13], numerous studies attributing the main antibacterial mechanism of cerium dioxide to the direct contact between cerium dioxide and bacterial membranes due to the presence of oxygen vacancies according to Frenkel's interpretation (Frenkel defects) [14]. Besides, cerium dioxide exhibits a strong optical spectrum in the UV-visible region in the range (from 3 to 3.2 eV) [15]. The physical and chemical properties of cerium oxide can be modified by doping it with metal ions, such as copper ions (Cu^{2+}), which have an incomplete (orbital-d) and can retard photogenerated charges [16]. Due to the difference in atomic radii between copper and cerium, this facilitates precise control of the Cu^{2+} doping levels in cerium oxide. The oxygen vacancies are increased and the photoactivity is enhanced by adding copper ions to cerium oxide [17]. Cerium (58) when doped with copper (29) replacement of the cerium atom with a copper atom and thus the existence of a local vacuum due to the difference in the size of the cerium ion from the size of copper ion. This vacuum resulting from the replacement of an atom with an atom will be filled with new energy levels within the original energy gap of cerium oxide. When the compound is exposed to an electromagnetic spectrum, a local plasmon resonance will occur as a result of the formation of these new levels within the energy gap of cerium oxide. We clearly observe this when studying the optical absorption spectrum of cerium oxide as in paragraph (3.2).

Many chemical methods have been used to synthesize cerium oxide nanoparticles such as co-precipitation [18],

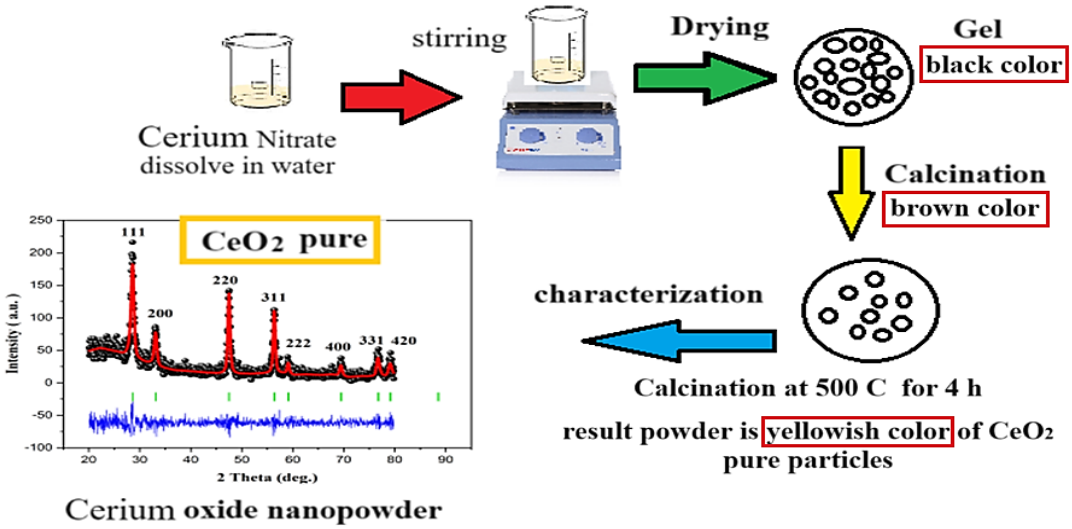

Fig. 1. Graphic abstract of pure cerium oxide powder preparation.

hydrothermal technique [19], sol-gel [20], electrodeposition [21] and thermal chemical spray method, hypergravity coprecipitation method etc. Among of these techniques, we have chosen sol-gel technique due to its low cost, easy to perform and environmental friendliness. In this work, cerium oxide doped with metal ion (Cu) at different concentrations (0.03, 0.06, 0.09), which was synthesized by sol-gel method, was investigated and its effect on its structure, morphology, photoactivity and antimicrobial properties against some bacteria. In addition, this review will give us an insight into the mechanism of action of cerium oxide nanoparticles as an antibacterial agent and help us open up prospects for its applications in future biomedical fields.

I. Experimental work

1.1. Preparation of CeO_2 nano powder

To prepare 5 g of cerium oxide nanopowder by sol-gel method according to the following steps (in laboratories of Ministry of Higher Education and scientific research, in Baghdad, Iraq*)*, 11.63 g of cerium nitrate $Ce(NO_3)_3.6H_2O$ (molecular weight=434.23 gm/mol) was dissolved in 100 ml of distilled water at a constant temperature of 70 °C for about three hours, then formed of a brown gel, the precipitate was dried overnight at 200 °C, thus forming a black particles. The prepared material was milled, and the next day it was calcined at 400 °C for four hours, thus forming a gray material, as shown in Figure 1 that observed sol gel steps [20] to produce high-purity of cerium powder.

The resulting material was milled again to obtain a fine powder, then calcined at 500 °C for four hours, Now the result powder is pure cerium oxide (according to XRD tests) in yellowish color. X-ray diffraction (XRD) was used to identify the crystalline phase and estimate the crystal size of the prepared compound. The previous steps are repeated in sequence for doping cerium oxide with copper using copper nitrate $Cu(NO_3)_23H_2O$ (molecular weight=241.6 gm/mol).

The preparation of cerium oxide by sol-gel method has an effective and clear effect in obtaining the smallest possible crystal size depending on the preparation temperature and calcination temperature. Since this research studies the bacterial effectiveness of cerium oxide, the smaller the particle size, the more we ensure that cerium oxide penetrates the cell wall, thus cell death. Where cerium oxide nanoparticles act as direct antioxidants and also act as free radical scavengers.

II. Results and discussion

2.1. Structural Properties Measurements:

2.1.1. X-ray diffraction:

The crystalline structure for any material can be recognized by studying the phase of (XRD) for that material. When a beam of (XRD) from wavelength incident on material surface, will exhibit peaks on limit angels for each material because of reflecting of Bragg on parallel crystalline surface. XRD instrument used in this research is of type (Shimad Zu 6000) made in Japan, with the following specifications: Target: Cu, Wavelength: 1.5406 A, Current: 30 (mA), Voltage: 40 (KV). The unit cell properties and purity of the crystalline phase of CeO_2 and Cu-doped cerium oxide nanoparticles (3%, 6%, and 9%) were analyzed via XRD diffraction, with results illustrated in figure 2. The prominent peaks in the patterns correspond to the (hkl) planes: (111), (220), (200), (222), and (311), respectively. These results indicate that the average sizes of CeO_2 and copper-doped cerium oxide nanoparticles at doping levels of 3%, 6%, and 9% were analyzed using XRD, yielding sizes of around 25 nm, 13 nm, 11 nm, and 17 nm, respectively.

No peaks indicative of a Cu-related impurity phase were found, suggesting that Cu has integrated into the CeO_2 matrix, as illustrated in figure 2. The average size of pure and copper-doped nanoparticles was calculated (as shown in table 1) from the XRD diffraction peak corresponding to the (111) plane using the Scherrer method, as presented in equation (1) [15]-[17].

$$D = \frac{0.9\ \lambda_{of\ XRD}}{\beta\ \cos\theta} \quad (1)$$

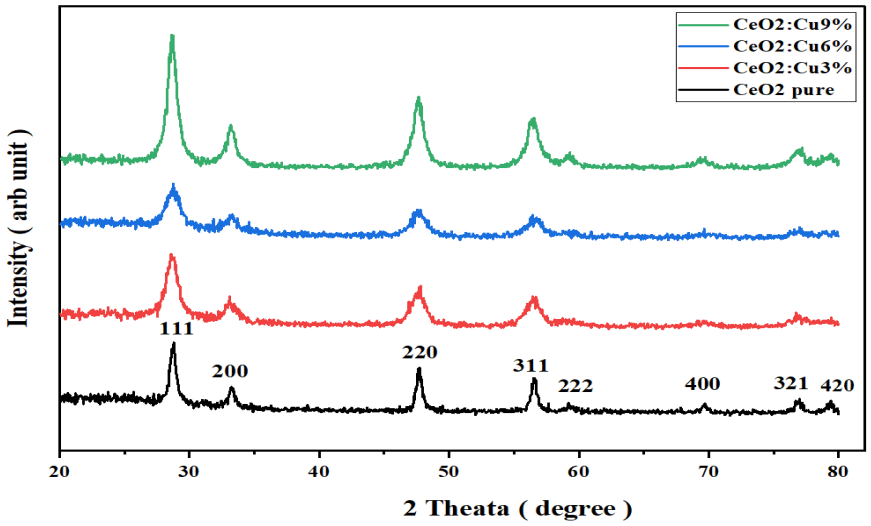

Fig. 2. XRD of Cerium Oxide pure and with different concertation of copper.

Table 1.

Parameter of XRD

Sample	Intensity	2Theata	FWHM	d-Spacing (A)	Crystallite size (nm)
CeO_2 pure	196	28.7618	0.5936	3.10146	25
CeO_2:Cu 3%	216	28.6836	1.1105	3.10974	13
CeO_2:Cu 6%	270	28.7605	1.2976	3.10160	11
CeO_2:Cu 9%	398	28.7047	0.8443	3.10750	17

Here, β is termed as FWHM (full- width at half maximum) and θ represents the angle of diffraction.

This change in intensity of peaks appears after the increase in the addition of copper, thus affecting the intensity of peak as observed in the figure 2, and this increasing in intensity is attributed to decrease in particle size after increase concentration of copper added as in table 1.

From Table 1, we can see the change in the intensity of the cerium oxide peaks after increasing the copper addition, and this increase in intensity is attributed to the decrease in particle size after increasing the added copper concentration as shown in Table 1, no peaks indicating the presence of an impurity phase associated with copper were found, indicating that copper has been incorporated into the cerium dioxide matrix, as shown in Figure 2.

The characteristics of CeO_2 are associated with its stable fluorite cubic (Fm3m) crystal structure. Cerium atoms are organized in a face-centered cubic (fcc) lattice, with each cerium atom encircled by eight oxygen atoms. Oxygen vacancies are generated within the lattice; the emergence of Ce^{3+} necessitates the creation of oxygen vacancies, which facilitate the production of CeO_2 and CeO_{2-x}. This characteristic enables cerium oxide nanoparticles to undergo redox reactions, allowing their application as catalysts for oxidation or reduction processes. The crystal sizes measured following the incorporation of copper into cerium oxide indicate that copper enhances the thermal stability of cerium dioxide. The X-ray diffraction parameters of the copper-doped sample indicate that the estimated crystal sizes diminish with increasing copper addition compared to the pure sample, signifying enhanced heat stability.

2.1.2. SEM Analysis:

The technology of Scanning Electron Microscopy (SEM) is one of the techniques used to study the size of particles accurately. SEM specifications used in this research is from type (MIRA III - Tescan) made in Czech, which specifications is: - Clarification power 3 nm, Magnification power of 80-300000 times, The type of images is either an image with secondary electrons or an image with background electrons, Accelerated voltage: from 50 to 30 kV. Figure 3 shows the scanning electron microscope images of cerium dioxide and cerium dioxide nanoparticles with copper addition. The resulting nanoparticles showed significant agglomeration. An increase in agglomeration was observed with the addition of copper. This confirms the significant reduction in crystallite size after the incorporation of copper ions into the cerium dioxide matrix, which in turn confirms the nanostructure of the resulting powder after the addition of copper.

It is noted that the addition of copper improved the physical properties in general, and this is evident in theSEM and TEM images and even in the X-ray diffraction analysis, as shown in Table 1, it is clear that the grain size decreased significantly as the copper concentration increased, and this is due to the copper filling the cerium vacancies in the original crystal and thus the abundance of oxygen, which plays a major role in the structure and composition of the crystal.

2.1.3. TEM Analysis

The Transmission Electron Microscopy (TEM) technique relies on the transmission of electrons through the material sample under investigation. It is distinguished by its high precision in measuring the dimensions of various nanoparticles. The TEM employed in this research is a Zeiss-EM10C-100KV model manufactured in Germany. TEM analysis was conducted on CeO_2 and CeO_2:Cu nanopowders with varying concentration of Cu , indicate that most particles are approximately 19 nm in size. Notably, an increase in doping results in a reduction

of particle sizes, as evidenced by the particle size histogram presented in Figure 4.

This result approximately appears to be consenting with XRD. Further substantiation the cubical phase of CeO_2 powder and its phase groups, this is in good agreement with literature data in introduction.

This result approximately appears to be consenting with XRD. Further substantiation the cubical phase of CeO_2 powder and its phase groups, this is in good agreement with literature data in introduction. From SEM measurements, it is clear that copper impurities improve the crystal structure of cerium oxide. where copper has a smaller ionic radius than cerium, when cerium is replaced by copper, this resulting void is filled with new energy levels to compensate for the difference in the size of the two atoms. These levels that are relied upon to improve the physical properties of cerium oxide in general.

2.1.4. FTIR Analysis

A Fourier Transform Infra Red (FTIR) spectrum is a modern technology that is used in both chemistry and physics, and can be used to determine the chemical and spectral properties of various materials, such as amino acids [18], where special absorptions of this type of amino occur in a specific area of the spectrum [19], the specifications of this instrument used in this research is type from (sgimadzu) made in Jaban, According to figure 6 within the range of 400-4000 cm^{-1} wavenumber which identify the chemical bonds as well as functional groups in the compound.

The large broad band at 3745 cm^{-1} is ascribed to the O-H stretching vibration in OH− groups. The absorption is peak around 1464 cm^{-1} is assigned to the bending vibration of C-H stretching. The intense band at 500 cm^{-1} corresponds to the Ce-O stretching vibration, as in table 2.

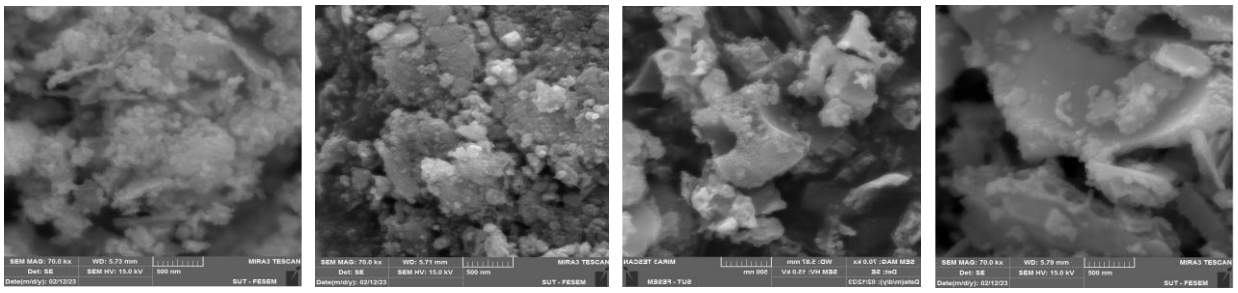

a) b) c) d)

Fig. 3. SEM magnified images of (a) pure cerium oxide, (b) CeO_2:Cu 3%, (c) CeO_2:Cu 6%, (d) CeO_2:Cu 9%.

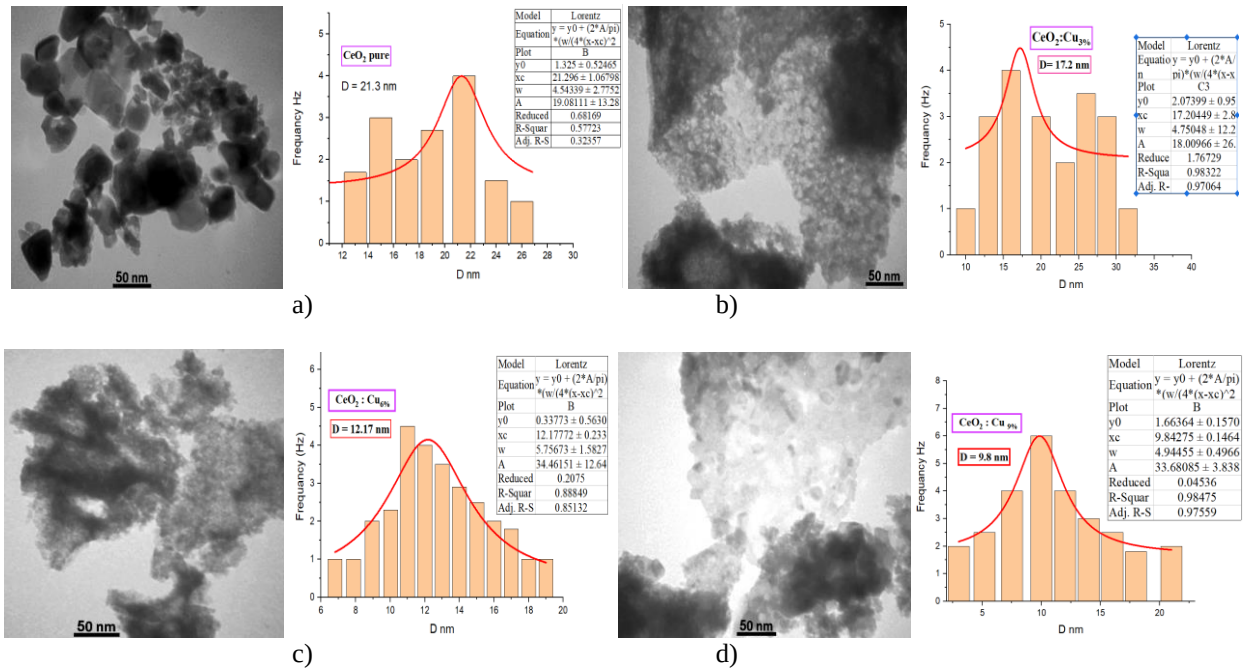

a) b) c) d)

Fig. 4. Grain size Diagnosis of TEM at 50 nm for (a) CeO_2 (b) CeO_2:Cu3% (c) CeO_2:Cu6% (d) CeO_2:Cu9%.

Table 2.

Peaks of vibration of FTIR spectrum

sample	Bonds				
	O-H	C-C	C-O	C=O	Ce-O
CeO_2 pure	3745.76	1577.7	744.52	694.37	883.4
CeO_2 : Cu 3%	3745.76	1577.7	748.38	690.52	852.54
CeO_2 : Cu 6%	3745.76	1570.06	--	694.37	848.68
CeO_2 : Cu 9%	3745.76	1516.05	744.52	--	852.54

The bands located at around 694.37, 744.52 and 1315.45 cm^{-1} have been attributed to the CO_2 asymmetric stretching vibration, CO bending vibration and C-O stretching vibration, respectively located at 1577.77 cm^{-1} are attributed to carbonate species vibrations and are clearly attenuated after calcination, indicating that the carbonate species have been decomposed by heat treatment. The FTIR spectra of CeO_2 nanoparticles prepared by sol-gel method with different reaction time are shown in figure 5. The bands at 545cm^{-1} and 750 cm^{-1} and 1379 cm^{-1} and 1539 cm^{-1} are due to the Ce – O stretching vibrations and the band at 3412 cm^{-1} is due to O-H vibration of water absorbed from the moisture.

From table 2 can be noted that carbon values in the CeO_2:Cu compound disappeared for all result ratios because of the thermal treatment of the compound.

2.2. Optical Properties Measurements

2.2.1. Absorption spectrum

UV-VIS spectroscopy serves as a highly efficient and widely employed method for characterizing nanoparticles, primari ly due to the relationship between their optical properties and various factors such as size, shape, and aggregation rate. The optical features of metal and metal-semiconductor nanostructures are significantly affected by localized surface plasmon resonance (LSPR) [20]. The reliability and ease of use of this technique render it a favored option for analyzing the properties of nanoparticles [21]. LSPR is defined by a pronounced increase in the absorption and scattering of light by nano-objects at a specific wavelength of incident light [22]. This phenomenon occurs when the incident light resonates with the natural frequency of electron oscillations on the surface of the nanostructure, as in figure 6. It is important to note that an increase in copper content results in a shift of the absorption maximum position in figure 6. This behavior is frequently observed in the spectra of nanocomposites where the size of the nanoparticles is approximately 100 nm [23]. Furthermore, the absorption peaks tend to shift towards the higher energy (shortwave) region due to the formation of more complex (aggregated) nanostructures [24]. The implications of these shifts are

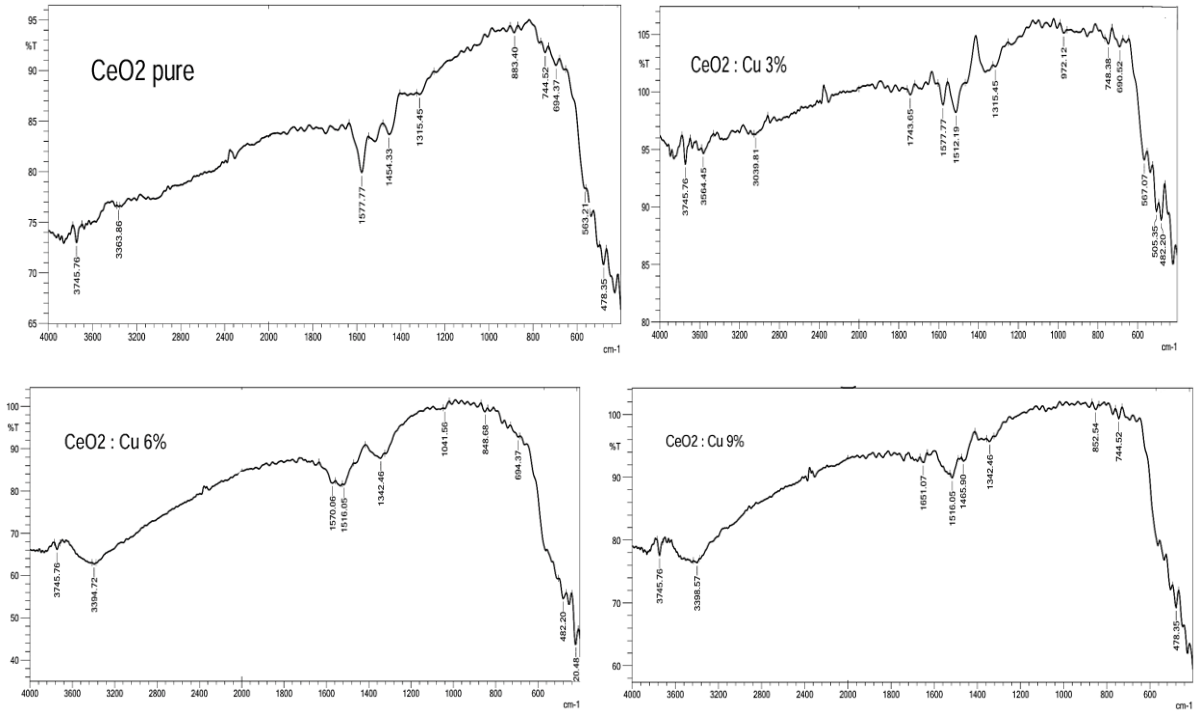

Fig. 5. FTIR Analysis of CeO_2 nanopowder before and after adding copper.

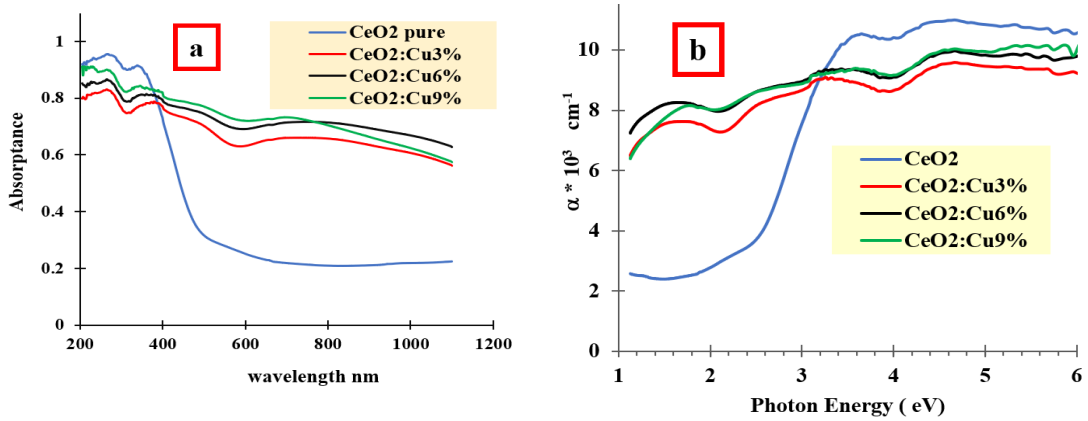

Fig. 6. (a) Absorptance spectrum (b) Absorption coefficient of CeO_2: Cu for various concentrations.

critical for understanding the optical behavior of nanoparticles in various applications. Overall, the insights gained from UV-VIS spectroscopy are invaluable for advancing the field of nanotechnology.

Figure (6-a) shows the absorption spectrum of pure CeO_2 nanopowder. It was observed that CeO_2 has two the absorption peaks are at the wavelength (249 nm and 351 nm), i.e. it has absorption spectrum in the UV region and visible region. It is noted that the absorbance decreases with increasing wavelength, and this behavior is due to the increase in the number of atoms and due to the spread of the nanoparticles, which leads to an increase in the number of collisions between the falling atoms [25], the reason of this phenomenon is cerium oxide probably having more than one activation energy (Ea), which in turn leads to an increase in the absorbance and thus an increase in the absorption coefficient, and thus leads to a reduction in the energy gap of the nanoparticles as in figure (6-a) shows a different absorption behavior of cerium oxide doping with copper, which is attributed to the localized surface plasmon resonance of CeO_2, this special behavior of nanopowder spectrum as it overlaps with the spectral patterns associated with two different crystal sizes [26], namely cerium and copper.

2.2.2. Absorption Coefficient Measurements:

Figure 6 shows the absorption coefficient spectrum of pure CeO_2 nanopowder. It was observed that the absorption edge is located at approximately the wavelength (542 nm), i.e. in the visible region. The observed absorption coefficient decreases with increasing wavelength, and Figure 6 shows that this expansion is interpreted as an overlap between the localized surface plasmon resonance (LSPR) patterns associated with the difference in crystal size between copper and cerium [27] and the changed absorption peak due to copper doping indicates a change in the band structure, where increasing doping concentration leads to the formation of bonds between copper and cerium [28]. It is noted that the density of defects in the crystal structure of cerium increases with the increase in the concentration of copper impurities, as the 9% sample has a larger absorption peak compared to the remaining concentrations because tiny size, thus leading to a smaller energy gap at this percentage ; as in table 3.

2.2.3. Energy gap measurements

The energy gap is obtained by the relationship between the square of the absorption coefficient and the photon energy $(\alpha h\upsilon)^2$ on the y-axis and the photon energy ($h\upsilon$) on the x-axis, to estimate the energy gap by drawing a tangent to the curve and the set of intersection with the x-axis [29], as shown in Fig. 7, the optical energy gap of pure CeO_2 and doped with Cu nanoparticles is shown, the direct Eg values as shown in table(3) were obtained for the Cu doped CeO_2 powder prepared with different concentrations (3%, 6%, 9%), respectively.

From the figures above, the effect of increasing copper impurities can be observed, as confining atoms within the band gap leads to periodic changes in the position of the atoms due to localized surface plasmon resonance patterns [14][8]. We also note from table (3) above that these defects resulting from the increased concentration of copper impurities formed within the

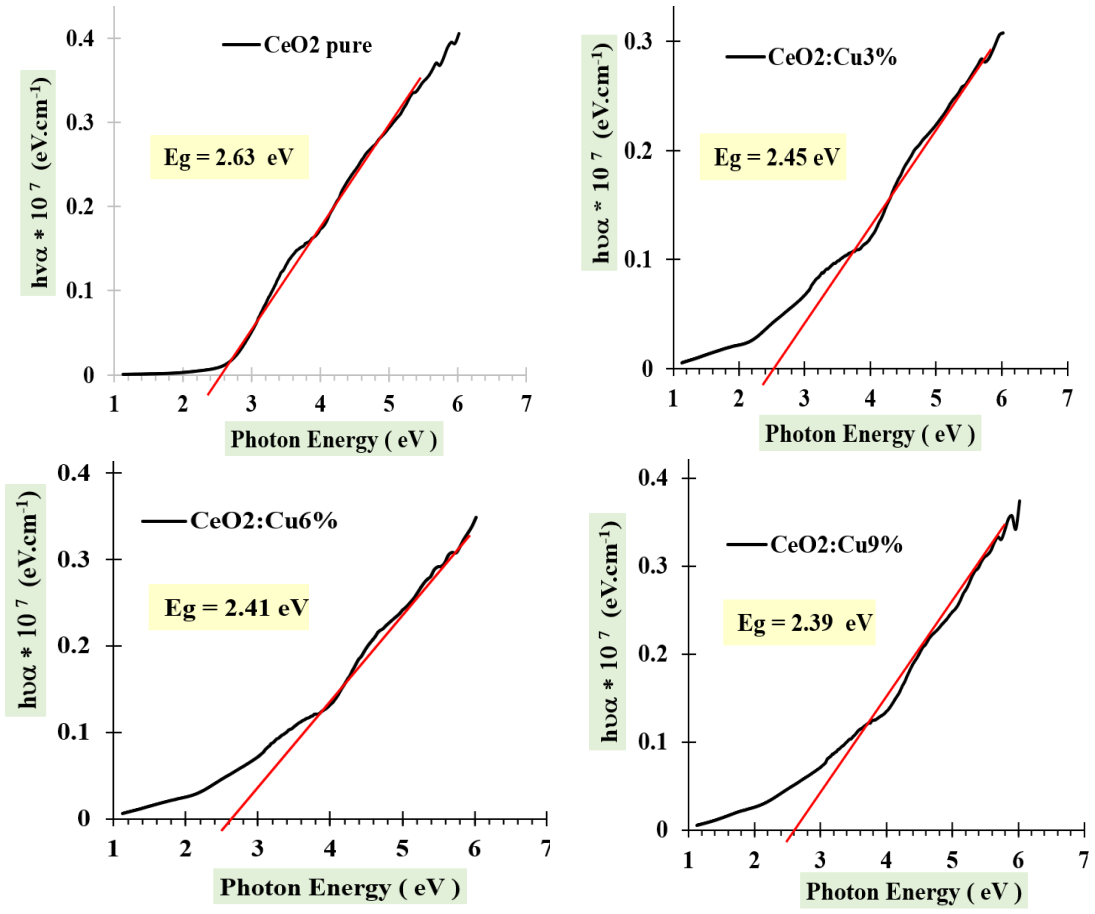

Fig. 7. Energy Band Gap of CeO_2: Cu for various concentrations.

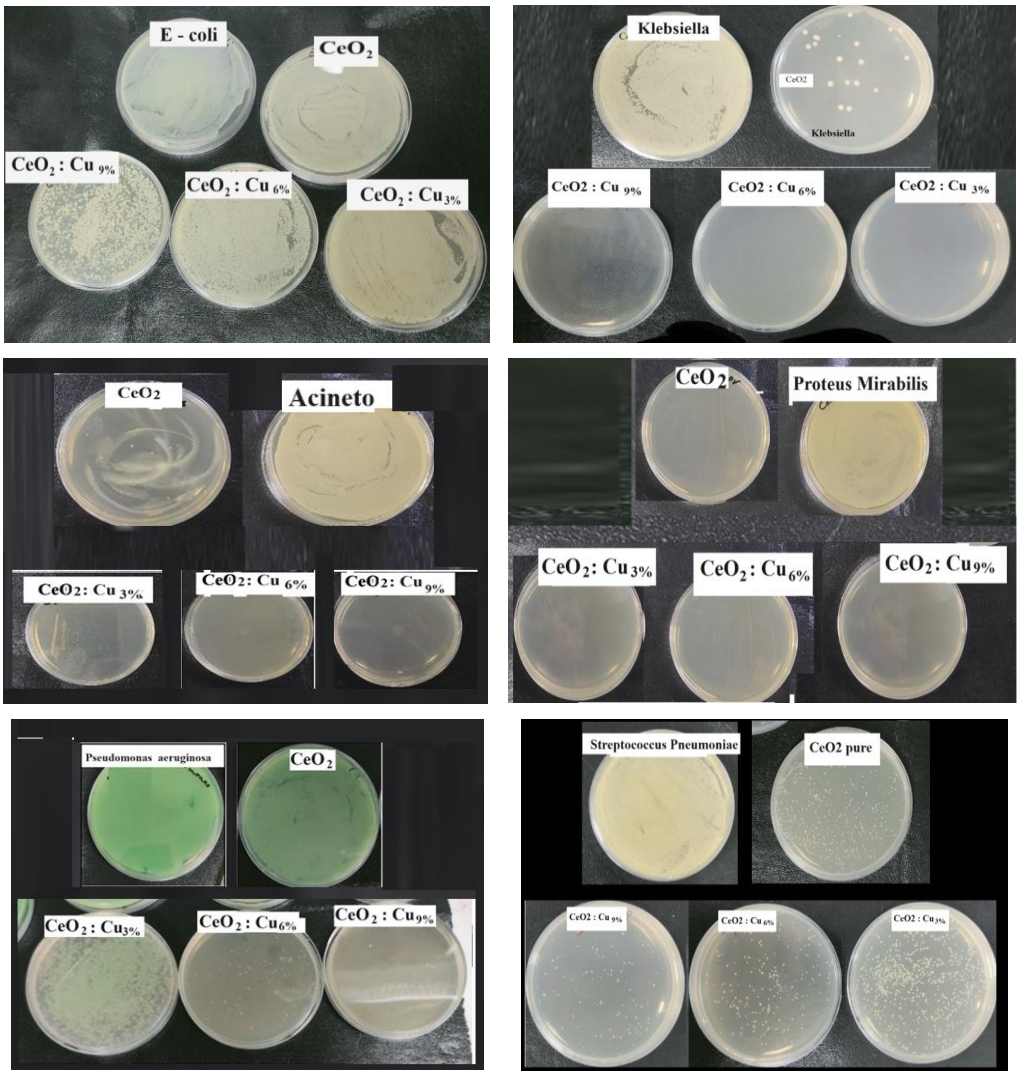

Fig. 8. Effect of CeO_2:Cu nanopowder against on gram-negative stain bacteria by liquid medium method.

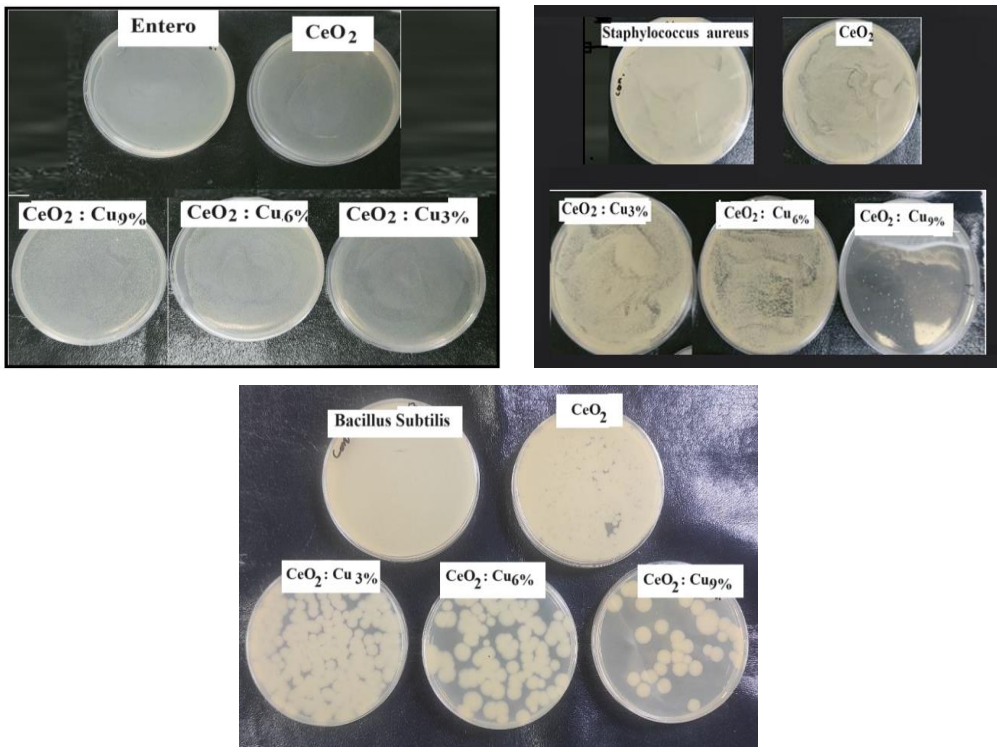

Fig. 9. Effect of CeO_2:Cu nanopowder against on gram-positive stain bacteria by liquid medium method.

direct band [17] led to a decrease in the band gap as shown in figure (7).

Table 3.

Relation between concentrations and energy gap of CeO_2: Cu nanopowder

Sample	concentrations	Eg eV
CeO_2	Pure	2.63
CeO_2:Cu	3%	2.45
	6%	2.41
	9%	2.39

This decrease is attributed to the formation of a new impurity level between the valence band level and the conduction band level, and this new level leads to a decrease in the energy gap after adding the impurities [21].

III. Antibacterial Tests

Many research have shown that cerium can be a long-lasting and efficient biocide against bacteria [30], it is safer for human cells [31] compared to other metal ions [32][33]. Cerium oxide powder's irregular form and rough surfaces damage bacterial membranes [34]. Also oxidative stress is crucial to cerium dioxide's antibacterial action [35]. Reactive oxygen species destroy nucleic acids, proteins, carbohydrates, lipids, and other biological components, impairing bacterial wall function and forcing cell death [36].

Figures 8 and 9 show the influence of CeO_2:Cu nanopowders prepared by mixing bacteria with these nanopowders on Gram-negative stains as in Figure 8 (such as Escherichia coli, Streptococcus pneumoniae, Proteus mirabilis, Acinetobacter baumannii, Pseudomonas aeruginosa, and Klebsiella pneumoniae) and on Gram-positive stains as in Figure 9 (such as Staphylococcus aureus, Enterococcus faecalis, and Bacillus cereus), this tests did in *laboratories of Ministry of Higher Education and scientific research, Scientific Research Authority, in Baghdad, Iraq*. Surprisingly, the 9% Cu nanoparticles exhibited the highest level of inhibition against all pathogenic bacteria. This indicates that the nanostructure of the cerium oxide powder is improved by the addition of Cu, thereby improving its antibacterial activity. Also, the metal oxide nanostructures exhibit a greater surface area than their bulk counterparts, which results in increased chemical and biological activity, as indicated by [37]. Based on these characteristics, metal oxide nanostructures can generally effectively target cell membranes to enhance bacterial inactivation [38]. To improve the battle against the rising drug resistance, however, extremely effective biomaterials must always be added to the original materials [39]. Consequently, multiple strategies are employed to achieve this, including the incorporation of impurities from other nanomaterials or the regulation of the size or structure of the prepared nanomaterials.

Form figure 8, its noted pure cerium oxide is good inhibition on gram-negative stain bacteria and it been better when added copper in Klebsiella and Proteus Mirabilis and Setreptococcus pneumonia and Acinetobacter, but pure cerium oxide is not good inhibition against E-coli and Pseudomonas aeruginosa bacteria and its tiny tine improved after increase adding copper, as shown in table 4, that agree with [23], [28], [30], [39].

From previous figure 9, its noted pure cerium oxide is good inhibition on gram-positive stain bacteria and it been better when added copper in Staphylococcus aureus and Bacillus cereus, but it was completely killing in Enterococcus faecalis, as shown in table 4, this agree with [33], [31], [34].

Conclusions

Cerium oxide nanoparticles were synthesized using a sol-gel method and doped with copper to enhance their properties. XRD diffraction showed a cubic fluorite structure, while SEM images showed spherical particles. UV-vis absorption data showed strong and a direct band gap 2.63 eV. The nanoparticles showed good antibacterial activity against six strains of negative bacteria and three strains of positive bacteria, cerium oxide vaccinated by 9% of copper nanoparticles showing the premium inhibition zone.

Hateef Areej Adnan – Msc degree in Physics;
Dhahri Essebti – Dr. degree in physics;
Mohammed Rasheed – Researcher in Applied Sciences Department;
Kadhim Habiba – Msc degree in Physics;
Abbas Zahraa – Msc degree in Biology;
Hassan Noor – Msc degree in Physics.

Table 4.

Effect of Cerium oxide on Negative and Positive Gram Bacteria behavior

Bacteria			Effect of CeO_2 nanopowder on growth of Bacteria			
			CeO_2 pure	CeO_2 : Cu 3%	CeO_2 : Cu 6%	CeO_2 : Cu 9%
Gram Negative	1	E - coli	non	non	non	low
	2	Streptococcus pneumoniae	good	good	good	high
	3	Proteus mirabilis	non	Completely killing	Completely killing	Completely killing
	4	Acinetobacter baumannii	High	Completely killing	Completely killing	Completely killing
	5	Pseudomonas aeruginosa	non	low	good	high
	6	Klebsiella pneumoniae	High	Completely killing	Completely killing	Completely killing
Gram Positive	1	Staphylococcus aureus	non	low	low	high
	2	Enterococcus faecalis	Completely killin	Completely killing	Completely killing	Completely killing
	3	Bacillus cereus	non	low	medium	high

[1] Y.C. Zhou, and M.N. Rahaman, *Synthesis and sintering of ultrafine CeO_2 powders*, Journal of Materials Research, 8, 1680 (1993).
[2] M. Nyoka, Y.E. Choonara, P.Kumar, P.P. D. Kondiah, V.Pillay, *Synthesis of Cerium Oxide Nanoparticles Using Various Methods: Implications for Biomedical Applications*, Nanomaterials (Basel), 10(2): article(242), 1 (2020); https://doi.org/10.3390/nano10020242.
[3] M. Farahmandjou, M. Zarinkamar,T.P. Firoozabadi, *Synthesis of Cerium Oxide (CeO_2) nanoparticles using simple CO-precipitation method*, Revista mexicana de física, 62(5), 496 (2016).
[4] K. Kaviyarasu, E. Manikandan, Z.Y. Nuru, M. Maaza, *Investigation on the structural properties of CeO_2 nanofibers via CTAB surfactant*, Materials Letters, 160, 61 (2015); https://doi.org/10.1016/j.matlet.2015.07.099.
[5] C. Martínez, C. Arcos, F. Briones, I. Machado, M. Sancy M. Bustamante, *The Effect of Adding CeO_2 Nanoparticles to Cu–Ni–Al Alloy for High Temperatures Applications*, Nanomaterials, 14(2), 143 (2024); https://doi.org/10.3390/nano14020143.
[6] K. Saravanakumar, M.M. Ramjan, P. Suresh, V. Muthuraj, *Fabrication of highly efficient visible light driven Ag/CeO_2 photocatalyst for degradation of organic pollutants*, Alloys and Compounds, 664, 149 (2016); https://doi.org/10.1016/j.jallcom.2015.12.245.
[7] K. Sakthiraj, B. Karthikeyan, *Synthesis and characterization of cerium oxide nanoparticles using different solvents for electrochemical applications*, Applied physics A, 126(52), (2020); https://doi.org/10.1007/s00339-019-3227-z.
[8] Paochi Chen, *Crystal Sizes and Energy Gaps of Cerium Oxide Using Co-Precipitation Method*, Materials Sciences and Applications, 13, 213 (2022); https://doi.org/10.4236/msa.2022.134012.
[9] Qiu Li Zhang, Zhi Mao Yang, Bing Jun Ding, *Synthesis of Cerium Oxide Nanoparticles by the Precipitation Method*, Materials Science Forum, 610-613, 233 (2009); https://doi.org/10.4028/www.scientific.net/MSF.610-613.233.
[10] P. Tamizhdurai, Subramanian Sakthinathan, Shen-Ming Chen, K. Shanthi, S. Sivasanker, P. Sangeetha, *Environmentally friendly synthesis of CeO_2 nanoparticles for the catalytic oxidation of benzyl alcohol to benzaldehyde and selective detection of nitrite*, Scientific Reports, 7 (46372), 1 (2017); https://doi.org/10.1038/srep46372.
[11] A. Dhouib, B.Mezghrani, G.Finocchiaro, R.Le Borgne, M.Berthet, B.Daydé-Cazals, A.Graillot, X.Ju, Jean-François Berret, *Synthesis of Stable Cerium Oxide Nanoparticles Coated with Phosphonic Acid-Based Functional Polymers*", Langmuir, 39(23), 8141 (2023); https://doi.org/10.1021/acs.langmuir.3c00576.
[12] K. Kandhasamy and K.Premkumar, *Fabrication of Cerium Oxide Nanoparticles with Improved Antibacterial Potential and Antioxidant Activity*, Bioscience Biotechnology Research Asia, 20 (2), 487 (2023); https://doi.org/10.13005/bbra/3104.
[13] M. Zandi, M.Fazeli, R.Bigdeli, V.Asgari, R.A.Cohan, R.Bahar, S.Shahmahmoodi, *Preparation of Cerium Oxide Nanoparticles and Their Cytotoxicity Evaluation In vitro and In vivo*, International Journal of Medical Toxicology and Forensic Medicine, 12(1), 1 (2022);
[14] Yu-Ming Chu, Muhammad Kamran Siddiqui, Sana Javed, Lubna Sherin, Farah Kausa, *On Zagreb Type Molecular Descriptors of Ceria Oxide and Their Applications*, Journal of Cluster Science, 3(33), 537 (2022); https://doi.org/10.1007/s10876-021-01984-y.
[15] K. Kashyap, F Khan, D Verma, S Agrawal Ch Chandra, P Kumar Dewangan, V Sahu, P R Verma, V K Jain, *Biofabrication and structural characterization of cerium oxide nanoparticles*, IOP Conference Series: Materials Science and Engineering, 1120, (2020); https://doi.org/10.1088/1757-899X/1120/1/012008.
[16] T. Arunachalam, M.Karpagasundaram, N.Rajarathinam, *Ultrasound assisted green synthesis of cerium oxide nanoparticles using Prosopis juliflora leaf extract and their structural, optical and antibacterial properties*, Materials Science-Poland, 35(4), 791 (2017); https://doi.org/10.1515/msp-2017-0104.
[17] Kryštof Skrbek, Ondřej Jankovský, *Synthesis and Characterization of Ceria Nanoparticles*, AIP Conference Proceedings, 2170, 020018-1 (2019); https://doi.org/10.1063/1.5132737.
[18] M. Pourhajibagher, N. Chiniforush, A. Bahador, Antimicrobial action of photoactivated C-Phycocyanin against Enterococcus faecalis biofilms: Attenuation of quorum-sensing system. Photo diagnosis and Photodynamic Therapy. 28, 286 (2019); https://doi.org/10.1016/j.pdpdt.2019.10.013.
[19] GarciaHeras, A.Jimenez, Morales, B. Casal, J.C. Galvan, S. Radzki, M.A. Villegas, *Preparation and electrochemical study of cerium–silica sol–gel thin films*, Journal of Alloys and Compounds, 380(1–2), 219 (2004); https://doi.org/10.1016/j.jallcom.2004.03.047.
[20] Xuanze Wang, *Preparation, synthesis and application of Sol-gel method*, Research Gate, 1 (2020)
[21] J. Calvache-Muñoz, FA. Prado, JE. Rodríguez-Páez, *Cerium oxide nanoparticles: synthesis, characterization and tentative mechanism of particle formation*, Colloids Surf A Physics chemistry and Engineering Aspects, 529, 146 (2017); https://doi.org/10.1016/j.colsurfa.2017.05.059.
[22] Ayad Shalaga Fudala, Waffa Mahdi Salih, Fatin Fadhel Alkazaz, *Synthesis different sizes of cerium oxide CeO_2 nanoparticles by using different concentrations of precursor via sol–gel method*, Materials today proceedings, 49(7), 2786 (2022); https://doi.org/10.1016/j.matpr.2021.09.452.
[23] M Qi, W Li, X Zheng, X Li, Y Sun, Y Wang, et al. *Cerium and its oxidant-based nanomaterials for antibacterial applications: a state-of-the-art review*. Front Mater, 7, 1 (2020); https://doi.org/10.3389/fmats.2020.00213.
[24] Y.H. Liu, J.C. Zuo, X.F. Ren, L. Yong, *Synthesis and character of Cerium oxide (CeO_2) nanoparticle by the precipitation method*, Metalurgija, 53(4), 463 (2014).
[25] R. Alvarez-Asencio, R.W. Corkeryb and A.Ahniyaz, *Solventless synthesis of cerium oxide nanoparticles and their application in UV protective clear coatings*, The Royal Society of Chemistry Advances, 10 (25), 14818 (2020); http://dx.doi.org/10.1039/D0RA01710H.

[26] M. S. Pujar, S.M. Hunagund, V. R. Desai, S.Patil , A. H. Sidarai, *One-step Synthesis and Characterizations of Cerium oxide Nanoparticles in an Ambient Temperature via Co-Precipitation Method*, American Institute of Physics, 050026, 1 (2017); https://doi.org/10.1063/1.5028657.

[27] J. Luňáček, O. Životský , P. Janoš, M. Došek, A. Chrobak, M. Maryško, J. Buršík , Y. Jirásková , *Structure and magnetic properties of synthesized fine cerium dioxide nanoparticles*. Journal of Alloys and Compounds, 753, 167 (2018); https://doi.org/10.1016/j.jallcom.2018.04.115.

[28] J. Gagnon, K.M. Fromm, *Toxicity and Protective Effects of Cerium Oxide Nanoparticles (Nanoceria) Depending on Their Preparation Method, Particle Size, Cell Type, and Exposure Route* ,European Journal of Inorganic Chemistry, 20(27), 4510 (2015); https://doi.org/10.1002/ejic.201500643.

[29] A. Fotopoulos, J. Arvanitidis, D. Christofilos, K. Papaggelis, M Kalyva, K. Triantafyllidis, D. Niarchos, N. Boukos, G. Basina, V. Tzitzios, *One pot synthesis and characterization of ultra fine CeO_2 and Cu/CeO_2 nanoparticles. Application for low temperature CO oxidation*, Journal of Nanoscience Nanotechnology, 11(10), 8593 (2011); https://doi.org/10.1166/jnn.2011.4752.

[30] O. L. Pop, A.Mesaros, D.C. Vodnar, R.Suharoschi, F.Tăbăran, L.Magerus, I.Sz. Tódor, Z. Diaconeasa, A.Balint, L.Ciontea and C. Socaciu, *Cerium Oxide Nanoparticles and their Efficient Antibacterial Application In Vitro against Gram-Positive and Gram-Negative Pathogens*. Nanomaterials, 10, 1 (2020); https://doi.org/10.3390/nano10081614.

[31] G. K. Ibadi, A. A. Taha, S. M. H. Al-Jawad, *Preparation and characterization of copper nanoparticles as antibacterial activity* , AIP Conference Proceedings, (3002(1), 030005 (2024); https://doi.org/10.1063/5.0206453.

[32] S. Ur Rehman, R.Khan Niazi, M. Zulqurnain, Q.Mansoor, J.Iqbal, A.Arshad, *Graphene nanoplatelets/CeO_2 nanotiles nanocomposites as effective antibacterial material for multiple drug-resistant bacteria*, Applied Nanoscience, 12, 1779 (2022); https://doi.org/10.1007/s13204-022-02422-9.

[33] F Abbas, J Iqbal, T Jan, N Badshah, Q Mansoor, M Ismail. *Structural, morphological, Raman, optical, magnetic, and antibacterial characteristics of CeO_2 nanostructures*. International Journal Miner Metal Matter , 23(1), 10 (2016); https://doi.org/10.1007/s12613-016-1216-1.

[34] G. Killivalavan, A.C.Prabakar, K. C.B. Naidu, B. Sathyaseelan, G. Rameshkumar, D. Sivakumar, K. Senthilnathan, I. Baskaran, E. Manikandan, B. R. Rao. *Synthesis and characterization of pure and Cu doped CeO_2 nanoparticles: photocatalytic and antibacterial activities evaluation*, Biointerface Research in Applied Chemistry, 10(2), 5306 (2020);

[35] N. Pandiyan, B.Murugesan J.Sonamuthu, S.Samayanan, S.Mahalingam, *PF_6 ionic liquid mediated green synthesis of ceramic SrO/CeO_2 nanostructure using Pedalium murex leaf extract and their antioxidant and antibacterial activities*, Ceramics International, 45(9), 12138 (2019).

[36] S. and M.Sánchez-Domínguez, *Synthesis of Mixed Cu/Ce Oxide Nanoparticles by the Oil-in-Water Microemulsion Reaction Method*, Materials, 9(480), 1 (2016); https://doi.org/10.3390/ma9060480.

[37] M. Martí, B.Frígols, A.Serrano-Aroca, *Antimicrobial Characterization of Advanced Materials for Bioengineering Applications*, Journal of Visualized Experiments, 138, 1 (2018); https://doi.org/10.3791/57710.

[38] M. Zhang, C.Zhang, X.Zhai, F.Luo, Y.Du, Chunhua Yan. *Antibacterial mechanism and activity of cerium oxide nanoparticles*, Sci China Mater, 62(11), 1727 (2019); https://doi.org/10.1007/s40843-019-9471-7.

[39] K. Zamani, N.oushin Allah-Bakhshi, F.Akhavan, M.Yousef, R.Golmoradi, M.Ramezani, H.Bach, S.Razavi, G.-R. Irajian, M.Gerami, A.Pakdin-Parizi, M.Tafrihi and F.Ramezani, *Antibacterial effect of cerium oxide nanoparticle against Pseudomonas aeruginosa*, BMC Biotechnology, 21(68) (2021).

[40] H. Kadhim Aity, E. Dhahri, M.Rasheed, *Optimisation, dielectric properties, and antibacterial efficacy of copper-grafted MgO nanoparticles synthesized via sol-gel method*, Ceramics International, https://doi.org/10.1016/j.ceramint.2024.10.324.

А.А. Хатіф[1], Е. Дахрі[2], М. Рашід[3], Х. Кадхім[1], З. Аббас[1], Н. Хассан[4]

Дослідження впливу різниці концентрації міді на властивості нанопорошку церію

[1] *Управління наукових досліджень, Міністерство вищої освіти та наукових досліджень, Багдад, Ірак, tona96943@gmail.com*
[2] *Лабораторія фізичних застосувань, коледж наук, Університет Сфакс, Туніс*
[3] *Відділ прикладних наук, Технологічний університет, Багдад, Ірак*
[4]*Dental Department, University of Kufa, Iraq*

Чистий нанопорошок оксиду церію CeO_2 готували золь-гель методом. Дослідження проводили для чистого порошку, а далі до нанооксиду церію додавали домішки міді в концентраціях 3%, 6% і 9% для покращення його структурних і оптичних властивостей, з метою досягнення найкращих фізичних характеристик. Підготовлені чисті та леговані зразки були протестовані як антибактеріальні засоби проти багатьох штамів як грампозитивних, так і грамнегативних бактерій. Результати цієї роботи показують, що нанопорошки CeO_2:Cu володіють значними антибактеріальними властивостями, оскільки вони продемонстрували найвищий рівень пригнічення різних патогенних бактерій, що передбачає майбутнє застосування CeO_2:Cu в нанобіотехнологіях як біоматеріал.

Ключові слова: Оксид церію, золь-гель, нанопорошок, енергетичний розрив, антибактеріальний ріст.